Regulation of Nuclear Pore Complex Conformation by IP_3 Receptor Activation

David Moore-Nichols, Anne Arnott, and Robert C. Dunn
Department of Chemistry, University of Kansas, Lawrence, Kansas 66045 USA

ABSTRACT In recent years, both the molecular architecture and functional dynamics of nuclear pore complexes (NPCs) have been revealed with increasing detail. These large, supramolecular assemblages of proteins form channels that span the nuclear envelope of cells, acting as crucial regulators of nuclear import and export. From the cytoplasmic face of the nuclear envelope, nuclear pore complexes exhibit an eightfold symmetric ring structure encompassing a central lumen. The lumen often appears occupied by an additional structure alternatively referred to as the central granule, nuclear transport complex, or nuclear plug. Previous studies have suggested that the central granule may play a role in mediating calcium-dependent regulation of diffusion across the nuclear envelope for intermediate sized molecules (10–40 kDa). Using atomic force microscopy to measure the surface topography of chemically fixed *Xenopus* laevis oocyte nuclear envelopes, we present measurements of the relative position of the central granule within the NPC lumen under a variety of conditions known to modify nuclear Ca^{2+} stores. These measurements reveal a large, ~9-nm displacement of the central granule toward the cytoplasmic face of the nuclear envelope under calcium depleting conditions. Additionally, activation of nuclear inositol triphosphate (IP_3) receptors by the specific agonist, adenophostin A, results in a concentration-dependent displacement of central granule position with an EC_{50} of ~1.2 nM. The displacement of the central granule within the NPC is observed on both the cytoplasmic and nucleoplasmic faces of the nuclear envelope. The displacement is blocked upon treatment with xestospongin C, a specific inhibitor of IP_3 receptor activation. These results extend previous models of NPC conformational dynamics linking central granule position to depletion of IP_3 sensitive nuclear envelope calcium stores.

INTRODUCTION

Nuclear pore complexes (NPC) are enormous, ~125 MDa protein channels that span the nuclear envelope (NE), forming conduits between nuclear and cytoplasmic spaces. These macromolecular complexes may contain over 150 different protein subunits, forming eightfold rotationally symmetric pores embedded within the nuclear envelope (Akey, 1991; Akey and Radermacher, 1993; Fahrenkrog et al., 2001; Forbes, 1992; Goldberg and Allen, 1993; Goldberg et al., 1997; Hinshaw, 1994; Kiseleva et al., 2000; Pante and Aebi, 1996). NPCs govern both nuclear import of endogenous modulators of gene expression as well as the export of RNA to the cytoplasm (Bustamante et al., 1995; Oberleithner, 1999; Oberleithner et al., 1996; Stolz et al., 2000). In addition to roles in normal cellular physiology, NPCs may also be targeted by viruses seeking to infiltrate the nucleus (Kasamatsu and Nakanishi, 1998; Nakanishi et al., 2001; Whittaker et al., 2000).

To date, much of what is known of the NPC architecture comes from electron microscopy (EM) investigations and, to a lesser extent, atomic force microscopy (AFM) studies. The former have provided a detailed view of the static structure of the NPC, whereas in vitro AFM has revealed a more dynamic picture of NPC morphology (Danker et al., 1997; Danker and Oberleithner, 2000; Fahrenkrog et al., 2001; Perez-Terzic et al., 1996, 1999; Rakowska et al., 1998; Schneider et al., 1995; Stoffler et al., 1999; Stolz et al., 2000; Wang and Clapham, 1999). Generally, such studies find that the NPC is comprised of at least three major structural elements: a cytoplasmic ring consisting of eight similar subunits, a nuclear ring also exhibiting eight subunits, and a structure that consists of a spoke-like array symmetrically occupying the NPC central lumen (Akey, 1995; Akey and Radermacher, 1993; Allen et al., 1997; Goldberg and Allen, 1995; Goldberg et al., 1997; Hinshaw, 1994; Kiseleva et al., 2000; Pante and Aebi, 1993, 1995). The cytoplasmic ring exhibits a nominal outer diameter of ~120 nm, with subunits often found in EM studies decorated with a series of filaments that extend into the cytoplasm. Subunits of the nuclear ring attach to a set of interconnected nucleoplasmic filaments collectively comprising a structure called the nuclear basket (Fahrenkrog et al., 2001; Pante and Aebi, 1996; Stoffler et al., 1999). The central spoke complex lay between the cytoplasmic and nucleoplasmic rings and possesses membrane-spanning domains contacting both the NPC central lumen and the cisternal space of the nuclear envelope. (Akey and Radermacher, 1993; Goldberg and Allen, 1993, 1996; Hinshaw, 1994).

Complex processes regulate both passive and active transport across the nuclear membrane. Active nuclear import requires specific nuclear localization sequences on transported molecules and often requires cytoplasmic factors that bind the cargo and facilitates their transport through the NPC channel. In contrast, passive transport

Submitted December 12, 2001, and accepted for publication April 10, 2002.

Address reprint requests to Robert C. Dunn, Department of Chemistry, University of Kansas, Lawrence, KS 66045. Tel.: 785-864-4313; Fax: 785-864-5396; E-mail: rdunn@ku.edu.

0006-3495/02/09/1421/08 $2.00

through the NPC does not require nuclear localization sequences on the transporting species or the help of soluble factors. The size of passively transported molecules ranges from that of freely permeable ions up to species of ~40 kDa. Whereas the passive transport of molecules smaller than 10 kDa across the nuclear envelope is driven by concentration gradients alone, evidence suggests that diffusion of species in the 10 to 40 kDa range can be regulated by intracellular calcium levels (Allen et al., 2000; Lee et al., 1998; Stehno-Bittel et al., 1995b, 1996). Specific depletion of nuclear envelope calcium stores by inositol triphosphate (IP_3)-sensitive ion channels has been shown by several groups to block the passive transport of these molecules into the nucleus (Lee et al., 1998; Stehno-Bittel et al., 1995a,b, 1996).

Interestingly, high-resolution electron microscopy and AFM studies often observe the presence of a mass in the central lumen of the NPC after depletion of the nuclear envelope calcium stores. This mass is alternately referred to as the "central granule," "central plug," or "transporter complex"(Goldberg and Allen, 1993; Perez-Terzic et al., 1996). EM studies suggest that the transporter complex may span the entire central lumen of the NPC, comprising a centrally tapered cylinder with globular domains at either end (Allen et al., 1996, 1997; Gant et al., 1998; Goldberg et al., 1992; Kiseleva et al., 2000; Rutherford et al., 1997). As the presence of the central granule was correlated with depletion of nuclear envelope calcium, it was suggested that changes in nuclear envelope permeability might result from changes in the position of central granule (Lee et al., 1998; Perez-Terzic et al., 1996, 1997; Wang and Clapham, 1999). Others, however, have questioned the physiological significance of the central granule (Fahrenkrog et al., 2001; Stoffler et al., 1999; Stolz et al., 2000). Some believe that the central granule may simply represent cargo caught in transit or structures such as the nuclear basket collapsing into the central lumen of the NPC (Fahrenkrog et al., 2001; Stoffler et al., 1999; Stolz et al., 2000).

Two groups have recently reported conflicting results for AFM measurements on unfixed nuclear envelopes under buffered conditions (Stoffler et al., 1999; Stolz et al., 2000; Wang and Clapham, 1999). Using a scheme that classified NPCs as either "open" or "closed," Wang and Clapham (1999) found that 80% of NPCs appeared "plugged" under calcium depleting conditions when viewed from the cytoplasmic side of the envelope. A two-state model of NPC conformation was proposed in which the central granule could adopt a "plugged" or "unplugged" state depending on cisternal calcium levels (Wang and Clapham, 1999). Similar AFM measurements on unfixed tissues carried out by Aebi and coworkers, however, found no evidence for calcium-dependent conformational changes on the cytoplasmic face of the NPC. Instead, they found that the morphology of the NPC on the nuclear face of the envelope was changed by altering external calcium concentrations. Based on their observations, Aebi and coworkers proposed an alternate model for calcium-mediated conformational changes in which changes in the nuclear basket assembly might modify passive diffusion through the NPC and explain the appearance of the central granule (Fahrenkrog et al., 2001; Stoffler et al., 1999; Stolz et al., 2000).

In an attempt to unify and extend these earlier studies, we report extensive measurements of the central granule position as a function of treatments known to alter nuclear calcium concentrations (Stoffler et al., 1999; Stolz et al., 2000; Wang and Clapham, 1999). These treatments included variations in calcium concentrations of bathing solutions, addition of ATP, and activation of nuclear IP_3 receptors with IP_3. Moreover, we examined the location of the central granule with varying degrees of IP_3 receptor stimulation produced by the IP_3 receptor agonist, adenophostin A (Mak et al., 2001; Takahashi et al., 1994). Treatments found to decrease nuclear cisternal calcium resulted in an apparent shift in the position of the central granule of NPC populations ~9 nm toward the rim of the NPC cytoplasmic ring. Pharmacological activation of IP_3 receptors by adenophostin A, revealed the magnitude of the shift to be concentration dependent, exhibiting an EC_{50} of ~1.2 nM. The shift in central granule position after IP_3 receptor activation was blocked by xestospongin C, a specific inhibitor of IP_3 receptor activation (De Smet et al., 1999; Gafni et al., 1997). In addition, activation of IP_3 receptors resulted in a decrease in the depth of NPCs (~10 nm) measured from the nuclear surface of the envelope. These results are consistent with the idea of a calcium sensitive conformational change in the NPC that alters its permeability. The role of specific NPC components in calcium sensing are discussed.

MATERIALS AND METHODS

Preparation of nuclear envelopes

Oocytes were removed from adult female *Xenopus* laevis (*Xenopus* Express, Homosassa, FL) following the procedure outlined by Marcus-Sekura (Marcus-Sekura and Hitchcock, 1987). Once removed, oocytes were placed in Barth's solution containing: 10 mM HEPES, 88 mM NaCl, 1 mM KCl, 0.82 mM $MgSO_4$, 0.33 mM $Ca(NO_3)_2$, 0.41 mM $CaCl_2$, and 200 units penicillin/streptomycin (Sigma-Aldrich, St. Louis, MO), adjusted to a pH of 7.4. If not used immediately, oocytes were stored at 4°C for no longer than 1 day.

Nuclei were removed from oocytes using precision forceps and cleared of cytoplasmic debris by several cycles of gently drawing the nuclei into and out of the tip of a Pasteur pipette. Once isolated, nuclei were transferred to a mock intracellular buffer solution containing either: 140 mM KCl, 2.99 mM $MgCl_2$, 10 mM HEPES at a pH of 7.2 (no added Ca^{2+}) or 90 mM KCl, 10 mM NaCl, 2 mM $MgCl_2$, 1.1 mM EGTA, 0.75 mM $CaCl_2$, 10mM HEPES at a pH of 7.32 (free Ca^{2+} ~200 nM) depending on treatment conditions (see Results). After a minimum of 10-min incubation, nuclei were transferred to 5-mL plastic petri dishes containing 4 mL of the specific treatment solution. Nuclei were maintained in treatment solutions for 10 min. Adenophostin A, D-myo inositol 1,4,5-triphosphate, and xestospongin C (Calbiochem, San Diego, CA) were all used without further purification.

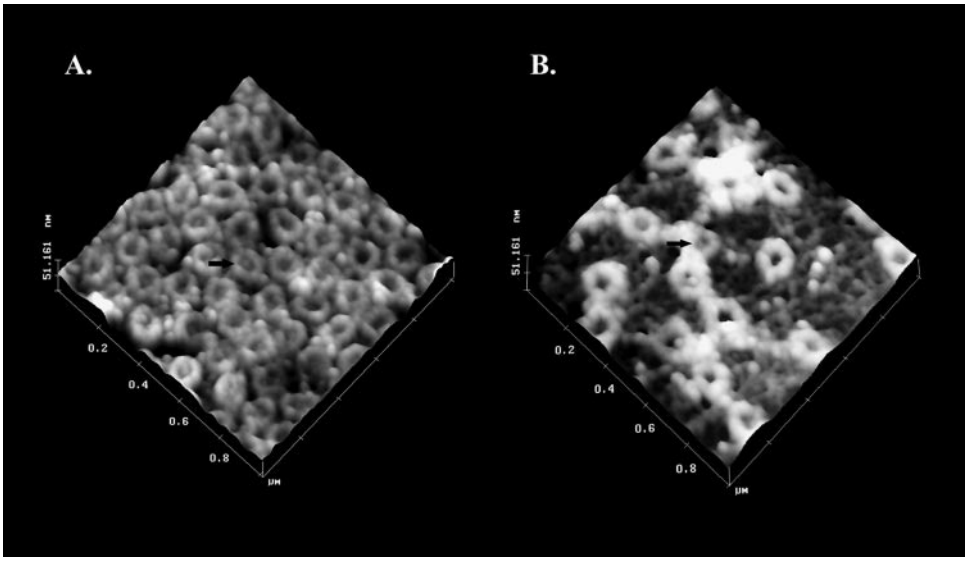

FIGURE 1 AFM images of the cytoplasmic (*A*) and nucleoplasmic (*B*) sides of the nuclear envelope. The 1.5 μm $\times$ 1.5 μm areas reveal the dense packing of NPCs in the membrane. (*A*) On the cytoplasmic side, many of the NPCs appear occluded by a mass known as the central granule (*arrows*). (*B*) On the nucleoplasmic side, the small filament lamin structures are clearly visible.

After the treatment period, intact nuclei were transferred to 12-mm glass coverslips and immersed in 5% paraformaldehyde prepared in an appropriate mock intracellular solution. The intact nuclei were incubated for 15 min after which they were gently pierced with two fire-polished glass micropipettes. Chromatin was teased out of the nuclei, and the membranes were carefully flattened onto the coverslip surface. Flattened membranes were rinsed twice in distilled water and air-dried. All treatment and fixation procedures were performed at room temperature (~23°C).

Atomic force microscopy

Atomic force microscopy measurements were performed using a Digital Instruments (Santa Barbara, CA) Nanoscope IIIa control station and multimode head. Sharpened silicon nitride AFM tips (Ultra-sharp, Micromasch, Tallinn, Estonia) with a nominal spring constant of 0.60 N/m were used in contact mode for all measurements. All AFM images used for analysis were collected on 1.5 μm $\times$ 1.5 μm sample areas at 512 $\times$ 512 pixel resolution.

To precisely extract the depth of the central granule within the NPC from the AFM data, topography images were analyzed using custom written macros running on a modified version of NIH Image (v1.62). For each NPC, 24 profile plots passing through the NPC center were collected at 7.5° intervals. Each set of 24 profile plots then was averaged together to produce a representative cross-section of each NPC. From this, the position of the central granule was calculated as the difference in height between the outer rim of the NPC and the top of the central granule.

RESULTS

Fig. 1 displays representative AFM images of the cytoplasmic (Fig. 1 *a*) and nucleoplasmic (Fig. 1 *b*) sides of the nuclear envelope. Great care was taken to insure that the appropriate side of the NE was imaged for a particular set of measurements because such ambiguities might be one source of the inconsistencies found in the literature. Nuclear membranes were carefully oriented on the surface manually and further checked for proper orientation using the AFM to identify distinct morphological markers. For instance, the nuclear face of the NE exhibits fibrous structures that stretch across the surface of the membranes (Fig. 1 *b*). These structures extend for tens of micrometers and are identified as lamin fibers in previous AFM and scanning electron microscope measurements (Goldberg and Allen, 1992, 1995, 1996; Schneider et al., 1995).

The fidelity maintained in the membrane structure was evidenced by a density of NPCs in the NE that is consistent with densities measured in other laboratories working with unfixed, native NEs. This suggests that the membrane preparation did not significantly alter the gross features of membrane morphology or modify the NPC distributions within the NE. The observation of small lamin fibers on the nuclear face of the membrane indicates that finer details of the NE were also preserved in the fixing process.

For these measurements, the pore depth was defined as the distance from the rim of the NPC to the top of the central granule. Large negative numbers reflected pores in which the granule was maximally recessed below the cytoplasmic ring of the NPC ("open"). An outward displacement of the central granule was reflected in pore depth measurements that evolved toward less negative or positive values ("closed").

Fig. 2 displays population histograms of the central granule position after the treatments indicated in the inset of the plots. The four histograms displayed in Fig. 2, *A* through *D*, result from measurements on nuclei subjected to various levels of ambient calcium. After preincubation, nuclei were incubated in modified mock intracellular solutions containing either 2 μM Ca^{2+} + 5 mM ATP, 2 μM Ca^{2+}, 200 nM

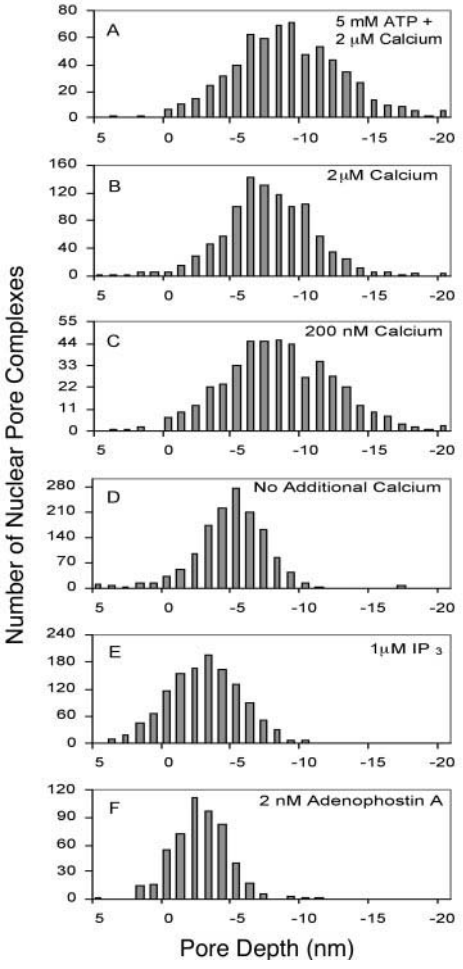

FIGURE 2 Population histograms of central granule location with the various calcium modifying treatments shown in the panel insets. Large negative numbers signify a recessed central granule position, a state identified as being "open." As seen in the histograms, treatments known to decrease the cisternal calcium levels shift the location of the central granule toward less negative numbers. These populations are identified with NPCs in a more "closed" state with the central granule shifted toward the cytoplasmic side of the NE.

Ca^{2+}, or the preincubation (nominally Ca^{2+} free) mock intracellular solution for 10 min and then fixed and imaged. After treatment with 2 μM Ca^{2+} + 5mM ATP (Fig. 2 *A*), the NPCs appeared in the most open configuration with the largest negative pore depth indicating that the central granule was recessed furthest from the rim of the NPC. The distributions were seen to gradually shift toward a more closed state (less recessed central granule) as the amount of ambient calcium was reduced.

The cisternal calcium can also be modified by specifically triggering the release of calcium through IP_3 receptors located in the NE. Previous reports on the effect of ambient calcium levels on IP_3 receptor activation concluded that IP_3 receptors are maximally active at ambient calcium concentrations of ~200 nM. (Stehno-Bittel et al., 1995a) To probe

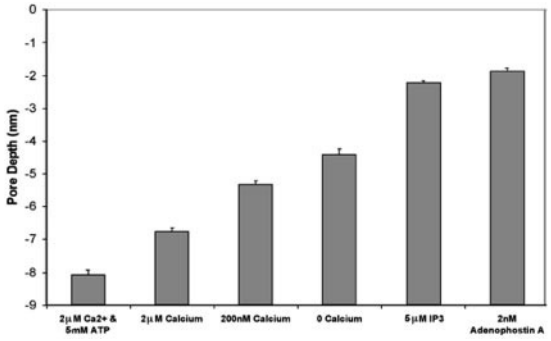

FIGURE 3 Average central granule location calculated from the population histograms shown in Fig. 2. The average pore depths after the various chemical treatments are: 2 μM Ca^{2+} + 5 mM ATP, average pore depth of 8.0 ± 0.2 nm (n = 647, in two nuclei); 2 μM Ca^{2+}, average pore depth of 6.8 ± 0.1 nm (n = 1014, in four nuclei); 200 nM Ca^{2+}, average pore depth of 5.3 ± 0.1 nm (n = 429, in one nucleus); nominally Ca^{2+} free mock intracellular buffer, average pore depth of 4.4 ± 0.2 nm (n = 202, in one nucleus); 1 μM IP_3, average pore depth of 2.2 ± 0.1 nm (n = 1256, in three nuclei); 2 nM adenophostin A, average pore depth of 1.9 ± 0.1 nm (n = 519, in one nucleus).

the effects of depleting nuclear cisternal calcium stores by IP_3 receptor activation, intact nuclei were preincubated in mock intracellular buffer containing 200 nM Ca^{2+} for 10 min. After incubation, nuclei were transferred to treatment solutions containing 1 μM IP_3 (with 200 nM Ca^{2+}) for another 10 min. AFM measurements on these NEs resulted in the depth histogram shown in Fig. 2 *E*.

IP_3 receptors were also stimulated by the addition of adenophostin A. Unlike IP_3, adenophostin A is more stable and less sensitive to functional regulation by enzymes controlling phosphatidyl inositol metabolism. Additionally, adenophostin A has been shown to exhibit a much greater potency in stimulating IP_3 receptor activation (Hotoda et al., 1999; Murphy et al., 1997). Fig. 2 *F* displays the central granule location histogram after incubation with 2 nM adenophostin A. The NPCs appear predominantly in the "closed" state with the central granule located near the NPC rim.

In general, the histograms displayed in Fig. 2 are structureless and reveal that the central granule can be positioned in a number of conformational states. This is evidenced by shifting distributions that move toward the "closed" state upon depletion of cisternal calcium. This is also seen in Fig. 3 in which the mean plug location and standard deviation calculated from the histograms shown in Fig. 2 are plotted. The bar graphs show the transition of central granule positions from the most "open" state at high calcium loading to the most "closed" state upon activation of the IP_3 receptors with either IP_3 or adenophostin A. The treatments and the respective measured pore depths are as follows: 2 μM Ca^{2+} + 5 mM ATP, average pore depth = 8.0 ± 0.2 nm (n = 647, in two nuclei); 2 μM Ca^{2+}, average pore depth = 6.8 ± 0.1 nm (n = 1014, in four nuclei); 200 nM Ca^{2+},

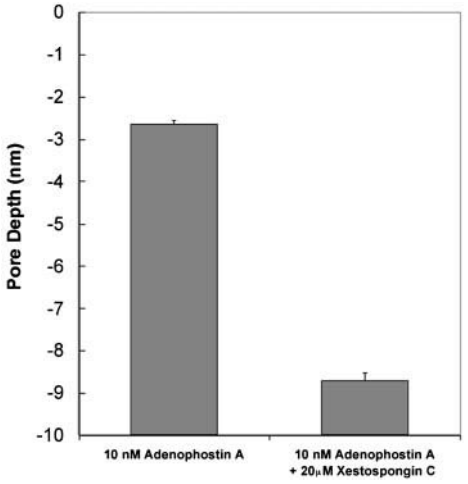

FIGURE 4 Adenophostin A induced displacement of central granule position. The average pore depths after adenophostin A treatment are: no added adenophostin A and 200 nM Ca2+, average pore depth of 5.3 ± 0.1 nm (n = 429, in one nucleus); 0.08 nM adenophostin A, average pore depth of 7.0 ± 0.1 nm (n = 550, in one nucleus); 0.4 nM adenophostin A, average pore depth of 6.8 ± 0.4 nm (n = 174, in one nucleus); 1.2 nM adenophostin A, average pore depth of 5.1 ± 0.1 nm (n = 522, in one nucleus); 2 nM adenophostin A, average pore depth of 1.9 ± 0.1 nm (n = 519, in one nucleus); 10 nM adenophostin A, average pore depth of 2.6 ± 0.1 nm (n = 547, in one nucleus); 250 nM adenophostin A, average pore depth of 3.0 ± 0.1 nm (n = 452, in one nucleus). The sigmoidal shaped dose-response curve reveals an EC_{50} of 1.2 nM, which is in close agreement with bulk measurements of adenophostin A activity.

average pore depth = 5.3 ± 0.1 nm (n = 429, in one nucleus); Ca^{2+} free mock intracellular buffer, average pore depth = 4.4 ± 0.2 nm (n = 202, in one nucleus); 1 μM IP_3, average pore depth = 2.2 ± 0.1 nm (n = 1256, in three nuclei); and 2 nM adenophostin A, average pore depth = 1.9 ± 0.1 nm (n = 519, in one nucleus).

The specific regulation of NPC conformation by IP_3 sensitive calcium stores was also explored. Using a specific pharmacological agonist of IP_3 receptors, adenophostin A, a dose-response relationship between IP_3 receptor activation and NPC conformation was examined. Fig. 4 plots the results of measured pore depths with increasing concentration of adenophostin A. It is important to note that in these experiments there was no difference in ambient calcium concentrations between treatments. Adenophostin A concentration was the only parameter varied. The dose-response curve reveals an ~EC_{50} of 1.2 nM adenophostin A. As shown in Fig. 5, the effects of adenophostin A activation of IP_3 receptors are blocked upon addition of 20 μM xestospongin C, a specific inhibitor of IP_3 receptor activation.

Finally, preliminary measurements on the nucleoplasmic side of the NE also revealed changes in NPC conformation upon activation of the IP_3 receptors. Fig. 6 compares the conformational changes observed on both the cytoplasmic and nucleoplasmic sides of the NPC after low and high doses of adenophostin A. The reported cytoplasmic and

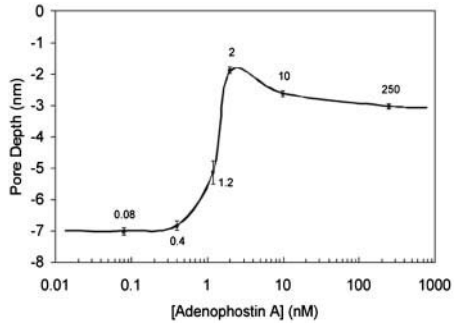

FIGURE 5 Comparison of average NPC pore depths after treatment with xestospongin C, a specific inhibitor of IP_3 receptor activation. Without xestospongin C, treatment of nuclei with 10 nM adenophostin A resulted in an average pore depth of 2.6 ± 0.1 nm (n = 547, in one nucleus). The combination of 10 nM adenophostin A and 20 μM xestospongin C, however, resulted in an average pore depth of 8.7 ± 0.2 nm (n = 470, in one nucleus). The significant difference in central granule location with xestospongin C treatment, suggest a specific functional link between IP_3 receptor activation and NPC conformational state ($p < 0.01$).

nucleoplasmic channel depths are measured relative to the cytoplasmic or nucleoplasmic rim of the NPC, respectively.

After treatments with 80 pM adenophostin A, the pore depths measured from the cytoplasmic and nucleoplasmic faces yielded depths of 7.0 ± 0.1 nm, (n = 550, one nucleus) and 10.0 ± 0.4 nm, (n = 270, one nucleus), respectively. After 10 nM adenophostin A treatments, pore depths measured from the cytoplasmic and nucleoplasmic faces, respectively, yielded values of 2.6 ± 0.1 nm (n = 547, one nucleus) and 3.3 ± 0.1 nm (n = 509, one nucleus). Interestingly, both sides of the NPC appear "unblocked" at

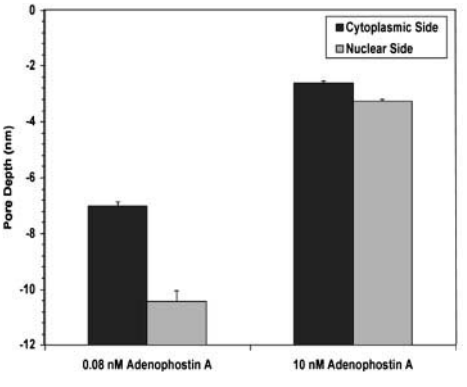

FIGURE 6 Comparison of pore depths taken on the cytoplasmic and nucleoplasmic NE surfaces for two different dosing levels of adenophostin A. The reported depths are taken relative to the respective rim of the NPC. At dosing levels of 0.08 nM adenophostin A, NPCs on the cytoplasmic side had an average pore depth of 7.0 ± 0.1 nm (n = 550, in one nucleus) and 10.5 ± 0.4 nm (n = 270, for one nucleus) for the nucleoplasmic face. At the higher dosing level of 10 nM adenophostin A, NPCs on the cytoplasmic side had an average depth of 2.6 ± 0.1 nm (n = 547, in one nucleus), whereas those on the nucleoplasmic side had an average depth of 3.3 ± 0.1 nm (n = 509, for one nucleus). Interestingly, upon depletion of cisternal calcium, both sides appear more occluded.

low adenophostin A concentrations and both appear "blocked" at high concentrations.

DISCUSSION

The role of calcium in modifying the permeability of the NPC continues to be a subject of some debate in the literature (Greber and Gerace, 1995; Santella and Carafoli, 1997, 1999). Early measurements suggested that calcium induced conformational changes in the NPC modulated permeability and that these changes were predominantly associated with the position of the central granule within the NPC (Perez-Terzic et al., 1996, 1997; Wang and Clapham, 1999). Recently, however, conflicting observations have questioned the validity of this mechanism (Fahrenkrog et al., 2001; Stoffler et al., 1999; Stolz et al., 2000). Those measurements have cast doubt on the role of the central granule in NPC permeability and its positional sensitivity to cisternal calcium levels. Often, however, the calcium treatments and conditions used in the various laboratories are not uniform, which makes comparisons problematic. One goal of the measurements reported here was to unify previous work by studying NPC conformation over a wide range of calcium modifying conditions.

The findings reported here unambiguously reveal a sensitivity of the central granule position to cisternal calcium levels. A systematic shift in the plug location toward the cytoplasmic face of the NPC was observed as the cisternal calcium levels were decreased. Moreover, specific activation of the IP_3 receptors in the NE with either IP_3 or adenophostin A resulted in a large shift in the central granule position toward the cytoplasmic face of the NPC. These receptors are known to release the cisternal calcium stores of the NE after activation (Lee et al., 1998; Stehno-Bittel et al., 1995a, 1996). This further supports a correlation between NPC conformational regulation and NE calcium stores.

It has been shown previously that 2 μM Ca^{2+} treatments combined with 5 mM ATP results in calcium uptake into NEs through the activation of membrane calcium transporters powered by ATP (Perez-Terzic et al., 1996; Stehno-Bittel et al., 1995a,b) As shown in Fig. 3, we find that this treatment results in the greatest number of pores in which the central granule is maximally recessed within the NPC complex. In the absence of ATP, treatments with 2 μM calcium alone resulted in populations exhibiting significantly less recessed positions of the central granule ($p < 0.01$). As the ambient calcium levels are further reduced, a transition in central granule position toward the cytoplasmic face of the NPC was observed (Figs. 2 and 3). These results reveal a sensitivity of the central granule location to the cisternal calcium levels and argue that the NPC can adopt a number of conformational states.

Studies have found that IP_3 receptors are abundant in the NE and are responsible for the release of the cisternal calcium stores (Mak and Foskett, 1994, 1997; Stehno-Bittel et al., 1995a) Moreover, stimulated depletion of nuclear calcium stores with IP_3 inhibits the passive transport of 10 kDa dextrans across the NEs of isolated, intact *Xenopus* nuclei (Greber and Gerace, 1995; Stehno-Bittel et al., 1995a, 1996).

This suggests a functional link between IP_3 receptor activation and NPC permeability. To further probe this link, NPC conformation state was characterized after treatments with IP_3, the physiological agonist of the receptor, and the more potent analogue adenophostin A. As shown in Figs. 2 and 3, both treatments resulted in the largest shift in the central granule location within the NPC. To establish pharmacological specificity, dose-response curves were measured after adenophostin A treatments.

Adenophostin A was chosen for the dose-response studies because, unlike IP_3, adenophostin A is less sensitive to functional regulation by enzymes controlling phosphatidyl inositol metabolism and is more potent in stimulating the release of intracellular calcium stores (Hotoda et al., 1999; Murphy et al., 1997). Fig. 4 shows the central granule location as a function of adenophostin A concentration. We find that increasing concentrations of adenophostin A does appear to drive a dose-dependent movement of the central granule toward the cytoplasmic face of the NPC. The sigmoidal shaped curve reveals EC_{50} of ~1.2 nM, which is consistent with bulk studies of adenophostin A activity (Adkins et al., 2000). Moreover, as shown in Fig. 5, treatments with xestospongin C blocked the action of adenophostin A. These observations argue for the pharmacological specificity of IP_3 receptor activation and its role in influencing the location of the central granule within the NPC.

Our data suggest a strong correlation exists between agonist-induced depletion of nuclear calcium stores and central granule position within the NPC cytoplasmic lumen. It appears likely, therefore, that the conformational changes observed by Wang and Clapham are indeed a consequence of IP_3 receptor-mediated depletion of NE calcium stores. Consistent with this, changes in the position of the central granule are also likely to be linked to mechanisms through which NPC permeability is regulated, as originally proposed (Lee et al., 1998; Perez-Terzic et al., 1996, 1997; Wang and Clapham, 1999). Our data, however, does not support a two-state model for central granule location. Instead, we find a shift in central granule location in response to calcium modifying treatments that reflects a distribution of available conformational states.

Preliminary measurements of NPC conformation on the nucleoplasmic side of the NE are compared with similar measurements made on the cytoplasmic side in Fig. 6. As seen in Fig. 6, large conformational changes in the NPC are observed on both sides of the NE after treatment with 10 nM adenophostin A. Interestingly, both sides of the NPC reveal a decrease in pore depth with release of NE cisternal calcium stores. This suggests a more complex mechanism of confor-

mational change than a simple unidirectional shifting of central granule location in response to cisternal calcium levels.

The large number of single pore measurements reported here reveal a shift in the central granule location as a function of treatments known to modify cisternal calcium levels. Moreover, the dose-response measurements shown in Fig. 4 suggest a pharmacological link between IP_3 receptor activity and the location of the central granule within the NPC. The identity of the central granule, however, remains unclear. Because AFM measurements, for the most part, reveal only topographical changes it is not easy to distinguish whether the central granule is an integral protein constituent of the NPC or simply cargo caught in transit. The dose-response measurements, however, suggest that at least some of the movement results from an integral component of the NPC structure. Moreover, the observation of a decrease in pore depth from both sides of the NPC with adenophostin A treatment suggest that the shifts are not entirely due to cargo. While cargo may be present, it is not likely that cargo alone would lead to the correlated variations in pore depth observed on both sides of the NE.

It should also be mentioned that if cargo is present, it might lead to variations in the pore depth measurements. This would tend to obscure structure otherwise present in the measured histograms. In other words, the histograms shown in Fig. 2 do not in themselves support a two-state model for central granule location. However, if these measurements represent a combination of both height information from central granule movement and that of cargo, then there may be specific substates in the central granule location that are not visible in the measured histograms.

Although the exact calcium depletion sensor in the NPC responsible for the central granule motion has not been identified, a likely candidate appears to be the Ca^{2+} binding protein gp210. This protein is present in each subunit of the eightfold symmetric NPC and contains Ca^{2+} binding motifs. Moreover, the role of gp210 in the passive permeability of the NPC has been implicated through studies in which antibodies raised to its lumenal domain have been found to inhibit passive diffusion. In addition, gp210 seems well suited structurally to act as a calcium sensor. It is a transmembrane protein with domains extending both into the cisternal region of the NE, where the calcium stores are located, and into the lumen of the NPC, where the central granule is observed (Greber and Gerace, 1992; Meier et al., 1995). Presumably, the domains found in the NE cisterna would act as the calcium sensor, and the domains extending into the NPC lumen would act as the effector. Measurements are currently underway to explore the role of gp210 in modulating NPC permeability.

CONCLUSIONS

The measurements reported here clearly show a correlation between nuclear cisternal calcium levels and conformation changes taking place within the NPC. Changes in the ambient calcium levels of the bathing solution as well as more specific modifiers of NE calcium are shown to result in changes in the position of the central granule. In general, treatments that lower the NE calcium levels result in a shift of the central granule toward the cytoplasmic side of the NPC. A similar shift toward the nucleoplasmic face of the NPC is also observed upon calcium depletion. In addition, a large change in the central granule location is observed after activation of IP_3 receptors with either IP_3 or the more potent and stable agonist adenophostin A. Dose-response curves of central granule location with adenophostin A treatments reveals a sigmoidal shaped curve with an EC_{50} of $\sim$1.2 nM. This response is blocked upon addition of xestospongin C, a specific inhibitor of IP_3 activity. Together these observations illustrate the pharmacological specificity of the conformational response and argue for the physiological coupling of IP_3 receptor activity and NPC permeability.

We gratefully acknowledge support for this work from National Institutes of Health (GM55290-01A2), the Alfred P. Sloan Foundation, and the Lila and Madison Self Foundation.

REFERENCES

Adkins, C. E., F. Wissing, B. V. Potter, and C. W. Taylor. 2000. Rapid activation and partial inactivation of inositol trisphosphate receptors by adenophostin A. *Biochem. J.* 352:929–933.

Akey, C. W. 1991. Probing the structure and function of the nuclear pore complex. *Semin. Cell Biol.* 2:167–177.

Akey, C. W. 1995. Structural plasticity of the nuclear pore complex. *J. Mol. Biol.* 248:273–293.

Akey, C. W., and M. Radermacher. 1993. Architecture of the Xenopus nuclear pore complex revealed by three- dimensional cryo-electron microscopy. *J. Cell Biol.* 122:1–19.

Allen, T. D., G. R. Bennion, S. A. Rutherford, S. Reipert, A. Ramalho, E. Kiseleva, and M. W. Goldberg. 1996. Accessing nuclear structure for field emission, in lens, scanning electron microscopy (FEISEM). *Scanning Microsc. Suppl.* 10:149–163.

Allen, T. D., G. R. Bennion, S. A. Rutherpord, S. Reipert, A. Ramalho, E. Kiseleva, and M. W. Goldberg. 1997. Macromolecular substructure in nuclear pore complexes by in-lens field- emission scanning electron microscopy. *Scanning* 19:403–410.

Allen, T. D., J. M. Cronshaw, S. Bagley, E. Kiseleva, and M. W. Goldberg. 2000. The nuclear pore complex: mediator of translocation between nucleus and cytoplasm. *J. Cell Sci.* 113:1651–1659.

Bustamante, J. O., A. Liepins, R. A. Prendergast, J. A. Hanover, and H. Oberleithner. 1995. Patch clamp and atomic force microscopy demonstrate TATA-binding protein (TBP) interactions with the nuclear pore complex. *J. Membr. Biol.* 146:263–272.

Danker, T., M. Mazzanti, R. Tonini, A. Rakowska, and H. Oberleithner. 1997. Using atomic force microscopy to investigate patch-clamped nuclear membrane. *Cell Biol. Int.* 21:747–757.

Danker, T., and H. Oberleithner. 2000. Nuclear pore function viewed with atomic force microscopy. *Pflugers Arch.* 439:671–681.

De Smet, P., J. B. Parys, G. Callewaert, A. F. Weidema, E. Hill, H. De Smedt, C. Erneux, V. Sorrentino, and L. Missiaen. 1999. Xestospongin C is an equally potent inhibitor of the inositol 1,4,5- trisphosphate receptor and the endoplasmic-reticulum Ca(2+) pumps. *Cell Calcium* 26:9–13.

Fahrenkrog, B., D. Stoffler, and U. Aebi. 2001. Nuclear pore complex architecture and functional dynamics. *Curr. Top Microbiol. Immunol.* 259:95–117.

Forbes, D. J. 1992. Structure and function of the nuclear pore complex. *Annu. Rev. Cell Biol.* 8:495–527.

Gafni, J., J. A. Munsch, T. H. Lam, M. C. Catlin, L. G. Costa, T. F. Molinski, and I. N. Pessah. 1997. Xestospongins: potent membrane permeable blockers of the inositol 1,4,5- trisphosphate receptor. *Neuron.* 19:723–733.

Gant, T. M., M. W. Goldberg, and T. D. Allen. 1998. Nuclear envelope and nuclear pore assembly: analysis of assembly intermediates by electron microscopy. *Curr. Opin. Cell Biol.* 10:409–415.

Goldberg, M. W., and T. D. Allen. 1992. High resolution scanning electron microscopy of the nuclear envelope: demonstration of a new, regular, fibrous lattice attached to the baskets of the nucleoplasmic face of the nuclear pores. *J. Cell Biol.* 119:1429–1440.

Goldberg, M. W., and T. D. Allen. 1993. The nuclear pore complex: three-dimensional surface structure revealed by field emission, in-lens scanning electron microscopy, with underlying structure uncovered by proteolysis. *J. Cell Sci.* 106:261–274.

Goldberg, M. W., and T. D. Allen. 1995. Structural and functional organization of the nuclear envelope. *Curr. Opin. Cell Biol.* 7:301–309.

Goldberg, M. W., and T. D. Allen. 1996. The nuclear pore complex and lamina: three-dimensional structures and interactions determined by field emission in-lens scanning electron microscopy. *J. Mol. Biol.* 257: 848–865.

Goldberg, M. W., J. J. Blow, and T. D. Allen. 1992. The use of field emission in-lens scanning electron microscopy to study the steps of assembly of the nuclear envelope in vitro. *J. Struct. Biol.* 108:257–268.

Goldberg, M. W., C. Wiese, T. D. Allen, and K. L. Wilson. 1997. Dimples, pores, star-rings, and thin rings on growing nuclear envelopes: evidence for structural intermediates in nuclear pore complex assembly. *J. Cell Sci.* 110:409–420.

Greber, U. F., and L. Gerace. 1992. Nuclear protein import is inhibited by an antibody to a lumenal epitope of a nuclear pore complex glycoprotein. *J. Cell Biol.* 116:15–30.

Greber, U. F., and L. Gerace. 1995. Depletion of calcium from the lumen of endoplasmic reticulum reversibly inhibits passive diffusion and signal-mediated transport into the nucleus. *J. Cell Biol.* 128:5–14.

Hinshaw, J. E. 1994. Architecture of the nuclear pore complex and its involvement in nucleocytoplasmic transport. *Biochem. Pharmacol.* 47: 15–20.

Hotoda, H., K. Murayama, S. Miyamoto, Y. Iwata, M. Takahashi, Y. Kawase, K. Tanzawa, and M. Kaneko. 1999. Molecular recognition of adenophostin, a very potent Ca2+ inducer, at the D-myo-inositol 1,4,5-trisphosphate receptor. *Biochemistry.* 38:9234–9241.

Kasamatsu, H., and A. Nakanishi. 1998. How do animal DNA viruses get to the nucleus? *Annu. Rev. Microbiol.* 52:627–686.

Kiseleva, E., M. W. Goldberg, J. Cronshaw, and T. D. Allen. 2000. The nuclear pore complex: structure, function, and dynamics. *Crit. Rev. Eukaryot. Gene Exp.* 10:101–112.

Lee, M. A., R. C. Dunn, D. E. Clapham, and L. Stehno-Bittel. 1998. Calcium regulation of nuclear pore permeability. *Cell Calcium.* 23: 91–101.

Mak, D. O., and J. K. Foskett. 1994. Single-channel inositol 1,4,5-trisphosphate receptor currents revealed by patch clamp of isolated Xenopus oocyte nuclei. *J. Biol. Chem.* 269:29375–29378.

Mak, D. O., and J. K. Foskett. 1997. Single-channel kinetics, inactivation, and spatial distribution of inositol trisphosphate (IP3) receptors in Xenopus oocyte nucleus. *J. Gen. Physiol.* 109:571–587.

Mak, D. O., S. McBride, and J. K. Foskett. 2001. ATP-dependent adenophostin activation of inositol 1,4,5-trisphosphate receptor channel gating: kinetic implications for the durations of calcium puffs in cells. *J. Gen. Physiol.* 117:299–314.

Marcus-Sekura, C. J., and M. J. Hitchcock. 1987. Preparation of oocytes for microinjection of RNA and DNA. *Methods Enzymol.* 152:284–288.

Meier, E., B. R. Miller, and D. J. Forbes. 1995. Nuclear pore complex assembly studied with a biochemical assay for annulate lamellae formation. *J. Cell Biol.* 129:1459–1472.

Murphy, C. T., A. M. Riley, C. J. Lindley, D. J. Jenkins, J. Westwick, and B. V. Potter. 1997. Structural analogues of D-myo-inositol-1,4,5-trisphosphate and adenophostin A: recognition by cerebellar and platelet inositol-1,4,5- trisphosphate receptors. *Mol. Pharmacol.* 52:741–748.

Nakanishi, M., T. Akuta, E. Nagoshi, A. Eguchi, H. Mizuguchi, and T. Senda. 2001. Nuclear targeting of DNA. *Eur. J. Pharm. Sci.* 13:17–24.

Oberleithner, H. 1999. Aldosterone and nuclear signaling in kidney. *Steroids.* 64:42–50.

Oberleithner, H., S. Schneider, and J. O. Bustamante. 1996. Atomic force microscopy visualizes ATP-dependent dissociation of multimeric TATA-binding protein before translocation into the cell nucleus. *Pflugers Arch.* 432:839–844.

Pante, N., and U. Aebi. 1993. The nuclear pore complex. *J. Cell Biol.* 122:977–984.

Pante, N., and U. Aebi. 1995. Toward a molecular understanding of the structure and function of the nuclear pore complex. *Int. Rev. Cytol.* 162B:225–255.

Pante, N., and U. Aebi. 1996. Molecular dissection of the nuclear pore complex. *Crit. Rev. Biochem. Mol. Biol.* 31:153–199.

Perez-Terzic, C., A. M. Gacy, R. Bortolon, P. P. Dzeja, M. Puceat, M. Jaconi, F. G. Prendergast, and A. Terzic. 1999. Structural plasticity of the cardiac nuclear pore complex in response to regulators of nuclear import. *Circ. Res.* 84:1292–1301.

Perez-Terzic, C., M. Jaconi, and D. E. Clapham. 1997. Nuclear calcium and the regulation of the nuclear pore complex. *Bioessays.* 19:787–792.

Perez-Terzic, C., J. Pyle, M. Jaconi, L. Stehno-Bittel, and D. E. Clapham. 1996. Conformational states of the nuclear pore complex induced by depletion of nuclear Ca2+ stores. *Science.* 273:1875–1877.

Rakowska, A., T. Danker, S. W. Schneider, and H. Oberleithner. 1998. ATP-Induced shape change of nuclear pores visualized with the atomic force microscope. *J. Membr. Biol.* 163:129–136.

Rutherford, S. A., M. W. Goldberg, and T. D. Allen. 1997. Three-dimensional visualization of the route of protein import: the role of nuclear pore complex substructures. *Exp. Cell Res.* 232:146–160.

Santella, L., and E. Carafoli. 1997. Calcium signaling in the cell nucleus. *FASEB J.* 11:1091–1109.

Schneider, S., G. Folprecht, G. Krohne, and H. Oberleithner. 1995. Immunolocalization of lamins and nuclear pore complex proteins by atomic force microscopy. *Pflugers Arch.* 430:795–801.

Stehno-Bittel, L., A. Luckhoff, and D. E. Clapham. 1995a. Calcium release from the nucleus by InsP3 receptor channels. *Neuron.* 14:163–167.

Stehno-Bittel, L., C. Perez-Terzic, and D. E. Clapham. 1995b. Diffusion across the nuclear envelope inhibited by depletion of the nuclear Ca2+ store. *Science.* 270:1835–1838.

Stehno-Bittel, L., C. Perez-Terzic, A. Luckhoff, and D. E. Clapham. 1996. Nuclear ion channels and regulation of the nuclear pore. *Soc. Gen. Physiol. Ser.* 51:195–207.

Stoffler, D., K. N. Goldie, B. Feja, and U. Aebi. 1999. Calcium-mediated structural changes of native nuclear pore complexes monitored by time-lapse atomic force microscopy. *J. Mol. Biol.* 287:741–752.

Stolz, M., D. Stoffler, U. Aebi, and C. Goldsbury. 2000. Monitoring biomolecular interactions by time-lapse atomic force microscopy. *J. Struct. Biol.* 131:171–180.

Strubing, C., and D. E. Clapham. 1999. Active nuclear import and export is independent of lumenal Ca2+ stores in intact mammalian cells. *J. Gen. Physiol.* 113:239–248.

Takahashi, M., K. Tanzawa, and S. Takahashi. 1994. Adenophostins, newly discovered metabolites of *Penicillium brevicompactum*, act as potent agonists of the inositol 1,4,5- trisphosphate receptor. *J. Biol. Chem.* 269:369–372.

Wang, H., and D. E. Clapham. 1999. Conformational changes of the in situ nuclear pore complex. *Biophys. J.* 77:241–247.

Whittaker, G. R., M. Kann, and A. Helenius. 2000. Viral entry into the nucleus. *Annu. Rev. Cell Dev. Biol.* 16:627–651.